EXPERIMENTAL STUDY ON THE EARLY STAGE OF UPWARD FLAME SPREAD WITH CROSS AIR FLOW

by

Zhongkai DENG, Jinfeng MAO [*], Zheli XING, Jin ZHOU

College of Defense Engineering, PLA University of Science and Technology, Nanjing, P.R. China

[*] Corresponding author; E-mail: maojinfeng628@163.com

In this work, experiments were conducted to study the upward flame spread with cross wind at an early stage (prior to the acceleration of pyrolysis spread rate of the wide slab). An exponential model was fitted to the experimental data of the spread rate of pyrolysis front and the dimensionless cross wind speed, which showed satisfactory results. The pyrolysis front tilt angle showed a decreasing trend with a low cross wind speed. However, at high cross wind speeds, the pyrolysis tilt angle exhibited an increasing trend with the maximum value of 45 °. The flame lengths increased with the cross wind for narrower slabs, whereas the phenomenon was most pronounced for the narrowest slab. Additionally, the flame length did not exhibit the lengthening phenomenon for the wider slab (0.1 m). Furthermore, the flame tilt angle did not exhibit significant change over time (even along the pyrolysis length). The correlation of flame tilt angle with the cross wind speed and width was also obtained in this study. The flame tilt angle presented a power-law increase with respect to the dimensionless cross wind speed.

Key words: *upward flame spread, cross wind, pyrolysis front, flame length*

1. Introduction

Upward flame spread is the most rapid and hazardous mode of flame spread [1], and therefore, is of significant interest in fire sciences [2, 3]. The upward flame is affected by several factors during its spread, including slabs width, sidewalls, altitude, and combustible material. Extensive research efforts have been devoted to investigate the influence of these factors on the upward flame spread. Pizzo et al. [3] performed experiments with slabs of 0.025-0.2 m width to study the effects of width on the spread of upward flame at an early stage. The results revealed that, for widths of greater than or equal to 0.1 m, the flame and the rate of spread were found to be width-independent. However, for the narrower slabs (0.025 and 0.05 m in width) a transition from laminar to turbulent was observed during the entire observation time. Nevertheless, Tsai [4-6] conducted a series of experiments using polymethyl methacrylate (PMMA) slabs of width 0.1-0.7 m with side walls, and observed width effects for the entire range of widths studied. Compared to flames without sidewalls, the existence of sidewalls produced higher flames and generally less heat feedback. These resulted in higher rates for the spread of flame for narrower flames, and vice versa. Liang et al. [7, 8] studied the effect of altitude on the spread of flame over PMMA slabs by conducting flame spread tests in Hefei (at an altitude of

29.8 m) and Lhasa (at an altitude of 3658.0 m). Compared with the results from Hefei, the lower ambient pressure in Lhasa transformed the delayed transition to a turbulent flow in a single stage of the flame spread process, whereas the flame spread rate was found to be about half of that in Hefei. Shih and Wu [9] studied the flame interaction effects on the spread of flame over multiple vertical cellulosic papers for a variety of configurations. The influence of a corner configuration on the upward flame was studied [10, 11], in which the pyrolysis front presented an "M"-like shape.

Most of the previous studies were conducted on the upward flame spread without considering any influence of the external wind. However, the upward flame spread with the external cross wind occurs frequently in fire scenarios. The external wind significantly influences the spread of flame. In this study, the upward flame spread with cross wind was studied experimentally. The experiments were conducted on PMMA slabs with widths of 0.025, 0.05 and 0.1 m, and at cross wind speed lying within the range of 0-1.2 m/s. Various influencing factors, such as the pyrolysis front spread rate, pyrolysis front tilt angle, pyrolysis front temperature gradient, flame length and flame tilt angle were analyzed.

2. Experimental

Figure 1 shows the schematic of experiment apparatus, which consists of a combustion platform and a wind tunnel. The wind tunnel had a variable speed fan, which produced stable longitudinal air flow. A piece of honeycomb cloth was installed about 2 meters from the fan to obtain uniform air flow within the wind tunnel. The combustion platform was placed at a distance of 0.3 m from the end of the tunnel. Furthermore, PMMA was used as the combustion slab due to its suitable thermo-physical properties. The PMMA slab was 12 mm thick, and was surrounded by a fire-proof board having the same thickness (12 mm). The fire-proof surface was kept flushed with PMMA slab in order to ensure the surface flame. The fire-proof board was fixed in a steel frame which was placed on a platform.

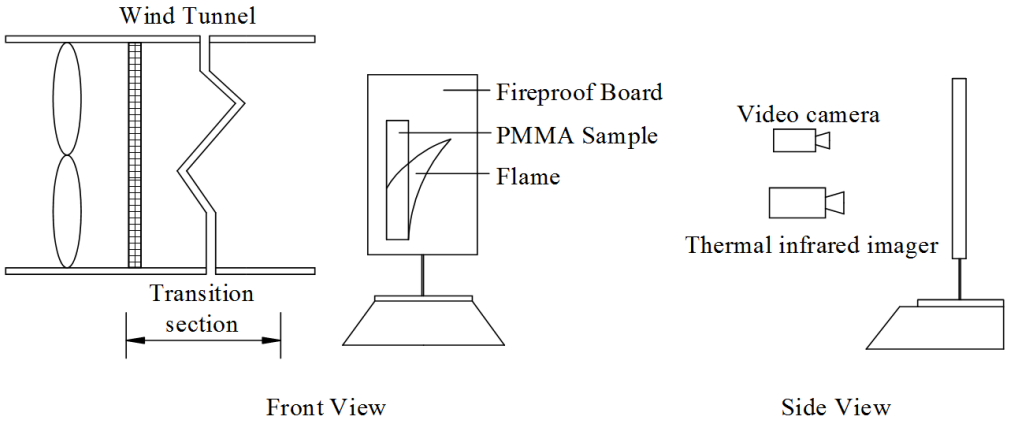

Figure 1. Schematic of the experimental setup

Three anemometers, each having the accuracy of ±0.01 m/s, were placed vertically parallel to the central line of PMMA slab to measure the cross flow air speed on the PMMA slab. The variable speed fan was adjusted to acquire certain air flow speeds (0.4, 0.8 and 1.2 m/s in this study) across the PMMA slab. The gears of the fan were recorded, and then, the anemometers were removed. When different experiments were performed, the fan was adjusted to the recorded gears to produce certain air flow speeds.

The surface temperature of the slab was recorded using the infrared camera, whereas the pyrolysis front was tracked as the temperature contour of 350 ℃. Even the temperature of the surface suffered from the effect of flame at the front of the slab. However, the determination of the pyrolysis front position was not significantly affected due to the reason that the temperature gradient was very high near the pyrolysis front. The rate of upward flame spread was determined by analysing the infrared video recordings of each experiment. The accompanying software allows the tracking of pyrolysis front as it moved upwards as the 350 ℃ contour. The method exhibited satisfactory accuracy, and was used extensively in previous researches [4, 6, 7, 12]. The infrared camera could work in the temperature range of -20 ℃ to 450 ℃ with the accuracy of ± 2 ℃ and the thermal sensitivity of less than 0.05 ℃. The imaging performance was in the form of 320×240 images, whereas the spatial resolution was 1.31 mRad. The geometrical characteristics of the flame were visualized using a camera with the film speed of 30 frames per second and image performance of 1280×720 (resolution).

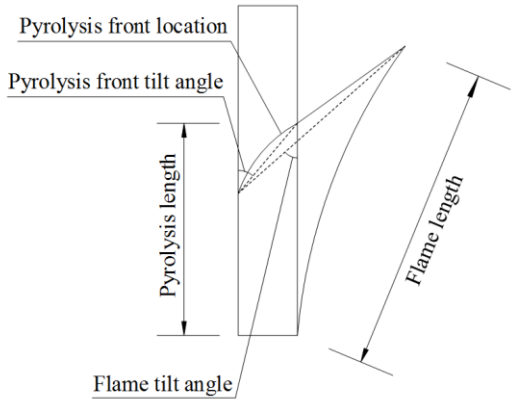

Figure 2. Flame characteristics

A steel tray with the cross section of 1 cm × 1 cm and length of 12 cm and with a rope soaked in ethanol was placed at the bottom of the PMMA slab to ignite it [8]. After the slab was ignited, the steel tray was removed. After the removal of steel tray, the flame was allowed to spread freely (without any external wind) for an additional 120 s to make the flame strong enough, so that it was not extinguished by the cross wind. Then, the fan of the wind tunnel was turned on to produce the cross wind. The time, when the fan was turned on, was taken as t = 0 s in this study. The flame characteristics are shown in Fig. 2.

3. Results and discussion

3.1. Pyrolysis front spread rate

Figure 3 shows the variation in pyrolysis length augment (for a better comparison, the pyrolysis length augment was taken as zero for t = 0 s in all of the cases) with time at different cross wind speeds for the slab widths considered. Fig. 3 demonstrates that the pyrolysis front spread rate decreased with the increase in cross wind. All cases showed a near-linear increase in the pyrolysis length, except for the width of 0.1 m at 0 m/s cross wind speed, which showed acceleration after about 220 s that is found to be in agreement with the results reported by Pizzo [3]. Fig. 4 shows the evolution of average pyrolysis rate in the observation time (as for the width of 0.1 m at 0 m/s cross wind speed, the time was taken before its acceleration) as a function of cross wind speed. Fig. 4 demonstrates that the narrower slabs (widths of 0.025 and 0.05 m) showed a similar trend. However, the wider slab (width of 0.1 m) exhibited a slightly different trend. The pyrolysis front spread rate exhibited only a slight decrease at the cross wind speed of 0.4 m/s. This was attributed to the fact that the flame tilt angle was small, which resulted in a nearly vertical spread. Fig. 5 shows the variation of pyrolysis front spread rate with the dimensionless cross wind speed (u^*), where $u^* = (u/gw)^{1/2}$. Here, u

represents cross wind speed, and *w* denotes the width of slab. The pyrolysis front spread rate exhibited an exponential decay with regards to *u**.

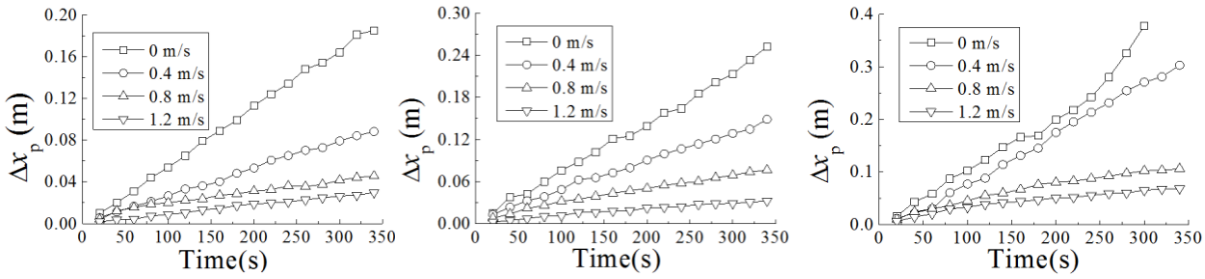

(a) *w* = 0.025 m (b) *w* = 0.05 m (c) *w* = 0.1

Figure 3. Variation of the pyrolysis length augment with time

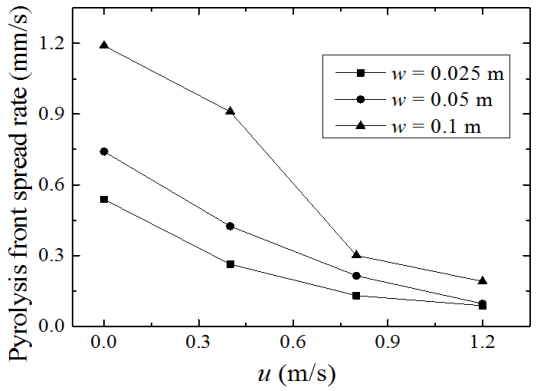

Figure 4. Variation of the pyrolysis front spread rate with cross wind speed

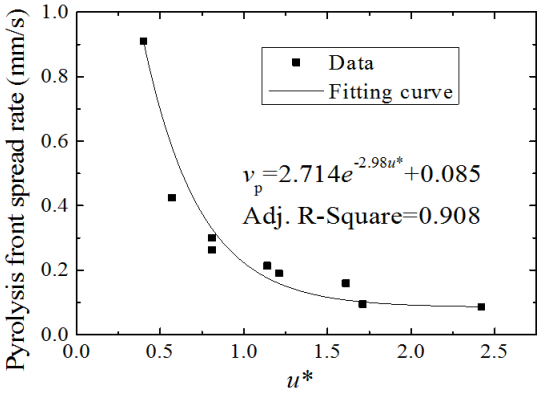

Figure 5. Correlation of the pyrolysis front spread rate with the dimensionless cross wind speed

3.2. Pyrolysis front tilt angle

The results for the pyrolysis tilt angle are shown in Fig. 2. The pyrolysis tilt angle was determined based upon the combined action of upright thermal buoyancy and external cross air flow. For the lighter cross air flow, the upright thermal buoyancy dominated, which resulted in a sharp cone-like pyrolysis front. Thus, the pyrolysis tilt angle decreased with time, as shown in Fig. 6(a). However, for the stronger cross air flow, the cross air flow dominated, which resulted in the side movement of the pyrolysis front vortex. Therefore, the pyrolysis tilt angle increased with time (see Fig 6(b) and (c)). In addition, the pyrolysis front tilt angle did not exceed 45 ° in the observed time, which was an unexpected phenomenon.

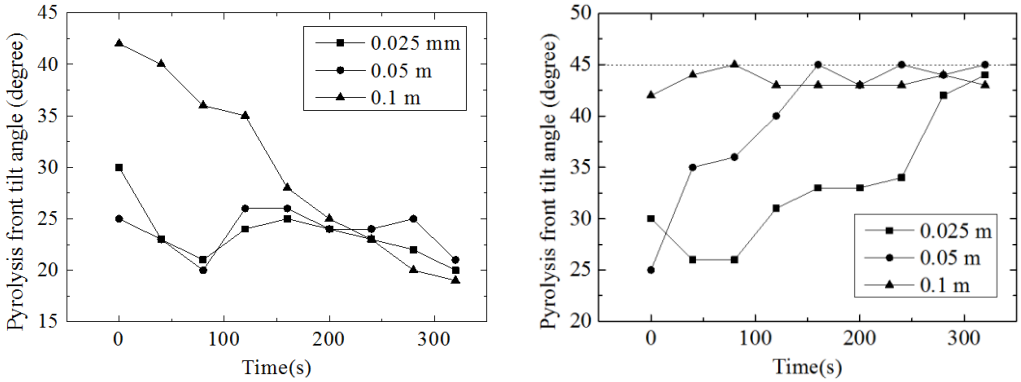

(a) *u* = 0.4 m/s (b) *u* = 0.8 m/s

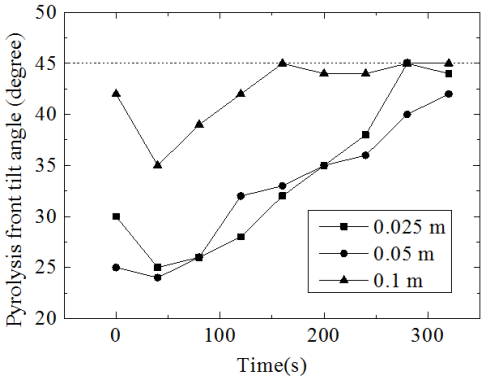

(c) u = 1.2 m/s

Figure 6. Variation of the pyrolysis front tilt angle with time for slabs of different widths

3.3. Pyrolysis front temperature gradient

Temperature gradient was defined according to Eq. (1) [13].

$$\text{Grad } T = \frac{\partial T}{\partial \vec{n}} \vec{n} \quad (1)$$

where $\vec{n}$ is the unit vector in the normal direction, and $\frac{\partial T}{\partial \vec{n}}$ is the temperature derivative in the normal direction of the point under consideration. The temperature gradient can be used to represent the preheating of flame. Furthermore, smaller the value of the gradient, stronger is the preheating, and vice versa. The temperature gradient can be calculated from the pyrolysis front line and the temperature contour above the pyrolysis front line according to Eq. (1). Fig. 7 shows the temperature gradient along the pyrolysis front line of the slab in the direction of wind. Fig. 7 shows that, without the cross wind, the temperature gradient was symmetrical about the central line of the slab. The temperature gradient decreased along the cross line of the slab in the cross wind direction for the case when the cross wind had a lower speed (0.4 m/s). However, for the cases of high cross wind speeds (0.8 and 1.2 m/s), the temperature gradient remained constant along the cross line of the slab. Moreover, the temperature gradient increased with the increased in wind speed, indicating that, with the growth of cross wind, the preheating weakened. Thus, when the cross wind speed increased, the pyrolysis front spread rate also decreased.

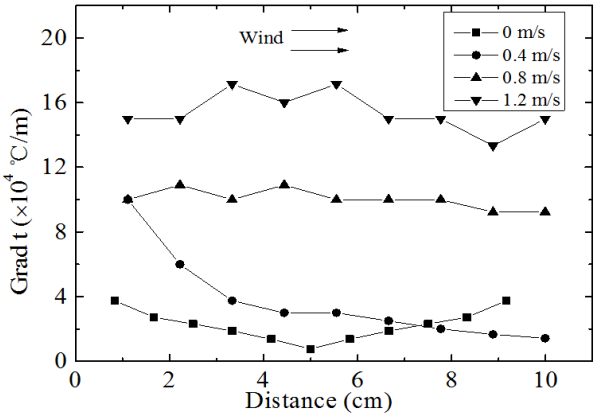

Figure 7. Temperature gradient along the pyrolysis front line in the direction of wind

3.4. Flame length

Figure 8 shows the relationship between the flame length and the pyrolysis length in the absence of cross wind. Previous studies have provided the correlation in the form: $x_{fl} = ax_p^n$ (where "a" and

"*n*" are constants) [14], and n = 0.802 [15], 0.781 [16], 0.7 [17], and 1 [18]. The correlation resulted from the results obtained in the current work is represented by Eq. (2).

$$x_{fl} = 3.0 x_p^{1.09} w^{0.25} \quad (2)$$

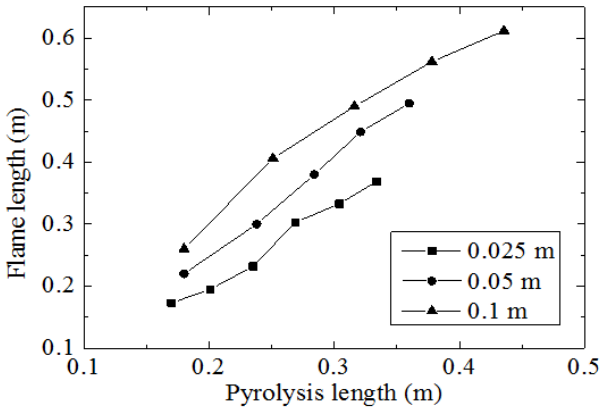

Figure 8. Flame length as a function of pyrolysis length

Tsai [7] considered the width effects, and suggested that: $x_{fl} \propto w^{0.2}$. Compared with the relationship: $x_{fl} \propto w^{0.25}$, the width effects in this study were more obvious, and were caused by the narrower slab used in the experiments. As for the influence of width, Rangwala et al. [19] addressed the mechanisms of width effects on the diffusion of fuel and the heat lost to the sides. The loss of fuel and heat to the sides was relatively significant for the narrower flame, and negligible for the wider flame. Tsai [4] provided a hypothesis addressing lateral air entrainment of the flame, which resulted in more efficient combustion, due to which, longer flame lengths were observed for wider flames.

Figure 9 shows the relationship between the flame and pyrolysis lengths in the presence of cross wind speed for the slabs of different widths. For the narrower slabs (widths of 0.025 and 0.05 m), the cross wind increased the flame length, as shown in Figs. 9(a) and (b). Moreover, Fig. 9(a) shows that the phenomenon is pronounced for the narrowest slab. The hypothesis put forward by Tsai [4] to explain the effects of width may illustrate the lengthening of flame. The cross wind can be considered as an additional lateral air entrainment, resulting in more efficient combustion and consequently, producing longer flame lengths. However, for the 0.025 m wide slab with cross wind speed of 1.2 m/s, slight lengthening of the flame was observed, which was shorter than those with the cross wind speeds of 0.4 and 0.8 m/s. This might be due to the reason that high cross wind take more heat from the flame. However, for the wider slab (0.1 m), the flame length did not show an increase with the increase in cross wind speed.

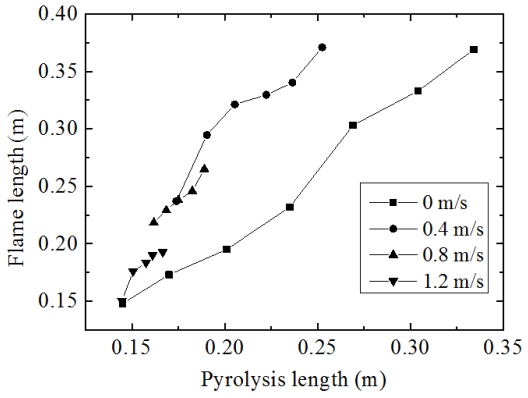

(a) w = 0.025 m

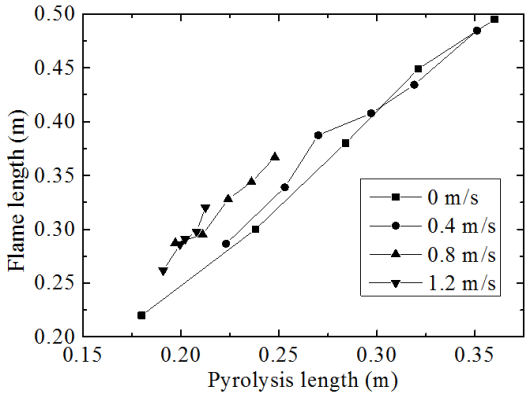

(b) w = 0.05 m

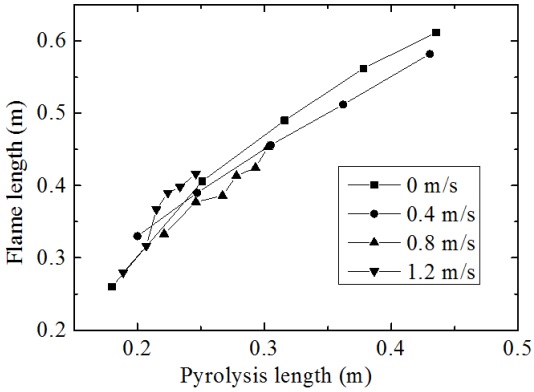

(c) w = 0.1 m

Figure 9. Flame length as a function of pyrolysis length

3.5. Flame tilt angle

The results for flame tilt angle are shown in Fig. 2. Fig. 10 shows the variation of flame tilt angle with time. As can be seen from Fig. 10, for all the cases studied, the flame tilt angle fluctuated with time. However, even with the fluctuations, the overall trend of the variation of flame tilt angle in the observed time remained almost constant. Fig. 11 shows the flame tilt angle (the value is the average of five values obtained during the time of observation) varied with the changes in cross wind speed. Fig. 11 demonstrates that the flame tilt angle increased with the increase in cross wind speed, and decreased with the increase in width. Eq. (3) correlates the flame tilt angle with the cross wind speed and the slab width.

$$\theta = 17.63u^{1.13}w^{-0.38} \tag{3}$$

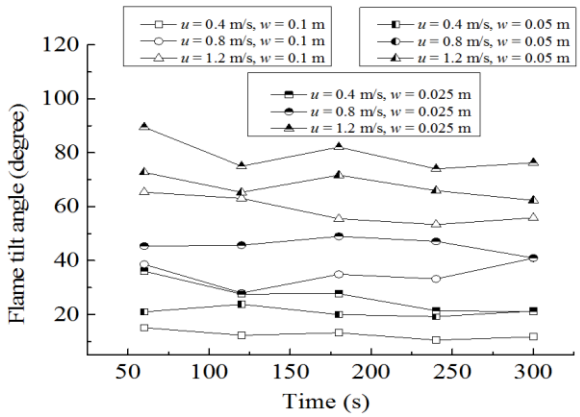

Figure 10. Variation of flame tilt angle with time

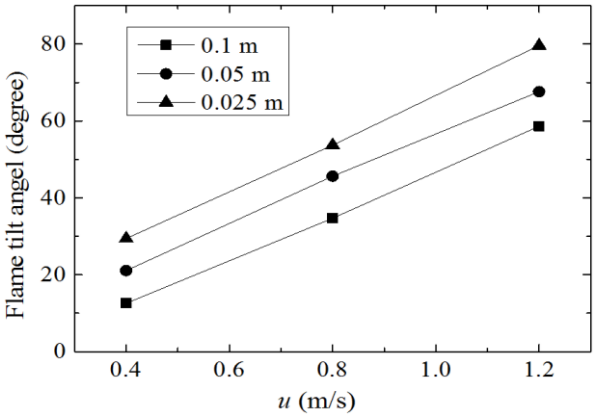

Figure 11. Variation of flame tilt angle with cross wind speed

Fig. 12 shows the variation in flame tilt angle with the dimensionless cross wind speed (u*). The results show that the flame tilt angle increased with the increase in u*. The results from curve fitting showed that an exponential function can satisfactorily represent the experimental data.

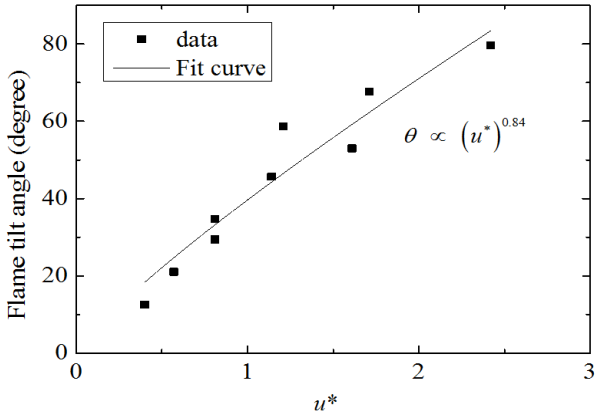

Figure 12. Correlation of the flame tilt angle with the dimensionless cross wind speed

4. Conclusions

In the present work, experiments were conducted to study the upward flame spread at different cross wind speeds at an early stage of the process. The slabs used in this study were 12 mm thick, and had the widths of 0.025, 0.05 and 0.1 m. The experiments were conducted at cross wind speeds of 0, 0.4, 0.8 and 1.2 m/s. Based upon the results obtained, following conclusions are drawn.

(1) The pyrolysis front spread rate reduced with the increase in cross wind speed, whereas the phenomenon was found to be more pronounced in the narrower slab. The pyrolysis front spread rate exhibited an exponential decay with the increase in dimensionless cross wind speed. The pyrolysis front showed different trends for different cross wind speeds. The pyrolysis front tilt angle showed a decreasing trend at low cross wind speeds, whereas, at higher cross wind speeds, the pyrolysis tilt angle exhibited an increasing trend with the maximum value of 45 °.

(2) The cross wind increased the flame length for the narrower slab, especially, for the narrowest slab. However, the lengthening of flame with cross wind did not occur in the wider slab (width of 0.1 m).

(3) The flame tilt angle increased with the increase in cross wind speed. However, the flame tilt angle decreased with the increase in the width of slab. The fitting results showed that a power function can satisfactorily represent the experiment data obtained for the flame tilt angle for different dimensionless cross wind speeds.

Acknowledgments

The authors greatly acknowledge the PLA University of Science and Technology for its support.

Nomenclature

a	constant, [-]
g	gravity acceleration, [m/s^2]
n	constant, [-]
t	time, [s]
T	temperature, [℃]
u	cross wind speed, [m/s]
u^*	dimensionless cross wind speed [= $(u/gw)^{1/2}$], [-]
v_p	pyrolysis front spread rate, [mm/s]
w	width of the slab, [m]
x_{fl}	flame length, [m]
x_p	pyrolysis length, [m]

Greek symbols

θ	deviation of flame tilt angle from the normal direction, [°]

Subscript

p	pyrolysis
fl	flame

References

[1] Leventon, I. T., Stoliarov, S. I., Evolution of flame to surface heat flux during upward flame spread on poly(methyl methacrylate), *Proceedings of the Combustion Institute*, *34* (2013), 2, pp. 2523-2530

[2] Brehob, E. G., *et al*., Numerical model of upward flame spread on practical wall materials, *Fire Safety Journal*, *36* (2001), 3, pp. 225-240

[3] Pizzo, Y., *et al*., Width effects on the early stage of upward flame spread over PMMA slabs: experimental observations, *Fire Safety Journal*, *44* (2009), 3, pp. 407-414

[4] Tsai, K. C., Width effect on upward flame spread, *Fire Safety Journal*, *44* (2009), 7, pp. 962-967

[5] Tsai, K. C., Wang, F. S., Upward flame spread: The width effects, *Proceedings*, Fire safety Science: Proceedings of the Eighth international symposium, Beijing, China, 2005, Vol. 8, pp.409-419

[6] Tsai, K. C., Influence of sidewalls on width effects of upward flame spread, *Fire Safety Journal*, *46* (2011) 5, pp. 294-304

[7] Liang, C., *et al*., Effects of altitude and inclination on flame spread over poly(methyl methacrylate) slabs, *Journal of Fire Sciences*, *31* (2013) , 6, pp. 511-526

[8] Liang, C., *et al*., Experimental study of vertically upward flame spread over polymethyl methacrylate slabs at different altitudes, *Fire & Materials*, *40* (2016), 3, pp. 472-481

[9] Shih, H. Y., Wu, H. C., An experimental study of upward flame spread and interactions over multiple solid fuels, *Journal of Fire Sciences*, *26* (2008), 5, pp. 435-453

[10] Cheng, Q., *et al*., Upward flame spread along pmma vertical corner walls part ii: mechanism of "m" shape pyrolysis front formation, *Combustion & Flame*, *99* (1994), 2, pp. 331-338

[11] Liang, C., *et al*., Experimental study on flame spread behavior along poly(methyl methacrylate) corner walls at different altitudes, *Journal of Fire Sciences*, *32* (2014), 1, pp. 84-96

[12] Pastor, E., *et al*., Computing the rate of spread of linear flame fronts by thermal image processing, *Fire Safety Journal*, *41* (2006), 8, pp. 569-579

[13] Holman, J. P., *Heat transfer*, McGraw-Hill Higher Education, New York, USA, 2010

[14] Consalvi, J. L., *et al*., On the flame height definition for upward flame spread, *Fire Safety Journal*, *42* (2007), 5, pp. 384-392

[15] Delichatsios, M. A., Flame heights in turbulent wall fires with significant flame radiation, *Combustion Science & Technology*, *39* (1984), 1, pp. 195-214

[16] Orloffa, L., *et al*., Upward turbulent fire spread and burning of fuel surface, *Proceedings*, Fifteenth Symposium (International) on Combustion, Tokyo, Japan, 1975, Vol. 15, pp. 183-192

[17] Tewarson, A., *et al*., Fire behavior of polymethylmethacrylate, *Combustion & Flame*, *89* (1992), 3-4, pp. 237-259

[18] Hasemi, Y., *et al*., Unsteady-state Upward Flame Spreading Velocity Along Vertical Combustible Solid And Influence Of External Radiation On The Flame Spread, *Proceedings*, Fire Safe Science: Proceedings of the Third International Symposium, Edinburgh, Scotland, 1991, Vol. 3, pp. 197-206

[19] Rangwala, A. S., *et al*., Upward flame spread on a vertically oriented fuel surface: the effect of finite width, *Proceedings of the Combustion Institute*, *31* (2007), 2, pp. 2607-2615